Hydromorphological implications of local tributary widening for river rehabilitation

M. Leite Ribeiro,[1,2] K. Blanckaert,[1,3] A. G. Roy,[4] and A. J. Schleiss[1]

Received 18 August 2011; revised 3 September 2012; accepted 5 September 2012; published 12 October 2012.

[1] The hydromorphological implications of the local widening of a tributary where it enters a confluence were investigated in a laboratory setting that is representative of the 20 major confluences on the channelized Upper Rhone River. Although local tributary widening reduces the confluence angle, it amplifies the hydromorphosedimentary processes in the confluence hydrodynamic zone (CHZ), because local widening reduces the effective flow area, causing increased tributary velocities and momentum flux. The reduction in effective flow area is caused by an increase in bed elevation and by lateral constriction of the flow induced by flow stagnation at the upstream corner of the confluence. The increased tributary velocities amplify the two-layer flow structure in the CHZ. Flow originating from the tributary is confined to the upper part of the water column and is more markedly directed outward than flow in the lower part of the water column originating from the main channel. A shear layer characterized by increased turbulence activity develops at the interface between the two flow layers. The increased tributary velocities enhance bed discordance, the penetration of the tributary into the CHZ and the channel bed gradients in the postconfluence channel. The results indicate that local tributary widening can enhance heterogeneity in sediment substrate, flow velocities and flow depths. Widening may therefore enhance local habitat and improve the connectivity of the tributary to the main river network. This may, in turn, provide favorable conditions for the improvement and reestablishment of ecological river functions, without having adverse impact on flood safety.

Citation: Leite Ribeiro, M., K. Blanckaert, A. G. Roy, and A. J. Schleiss (2012), Hydromorphological implications of local tributary widening for river rehabilitation, *Water Resour. Res.*, *48*, W10528, doi:10.1029/2011WR011296.

1. Introduction

[2] Many rivers have been channelized and regulated, often with the aim of flood protection and reclaiming land for urbanization and agriculture. These river training works often resulted in river systems with quasi-homogeneous flow and morphologic conditions, considerably reduced natural dynamics and impoverished biological communities of low ecological value [*Dynesius et al.*, 2004; *Dynesius and Nilsson*, 1994; *Formann et al.*, 2007; *Gurnell et al.*, 2009; *Lorenz et al.*, 1997].

[3] River confluences are strategic sites with respect to the ecological connectivity, flood safety and water quality. In natural conditions, these locations are typically characterized by high habitat heterogeneity, high variability in flow, sediment load, sediment size, which are requisites for high quality fluvial ecosystems. For those reasons, confluences may represent biological hotspots in river networks [*Benda et al.*, 2004; *Rice et al.*, 2006, 2008].

[4] River widening has become a common practice in river rehabilitation [*Formann et al.*, 2007; *Hunziger*, 1999; *Nakamura et al.*, 2006; *Rohde*, 2004; *Rohde et al.*, 2005; *Weber et al.*, 2009]. Its purpose is to allow the river to adjust to its natural dynamics and to enhance riparian and in stream habitat for plants and animals by increasing the heterogeneity in substrate, flow and morphology. As of yet, local widening of a tributary where it enters a confluence has not been investigated.

[5] This paper investigates the hydromorphological implications and the rehabilitation potential of local tributary widening by direct engineering intervention on rivers such as the Upper Rhone River, upstream of Lake Geneva, Switzerland (Figure 1). This river is channelized over almost its entire length at an almost constant embanked width. Also the lower reaches of the tributaries are channelized and the confluences are characterized by pronounced bed discordances (i.e., the difference in bed elevation between the tributary and the main channel at the tributary mouth), which have often been stabilized by means of weirs or block ramps. The natural

[1]Laboratory of Hydraulic Constructions, Ecole Polytechnique Fédérale de Lausanne, Lausanne, Switzerland.
[2]Stucky SA, Renens, Switzerland.
[3]State Key Laboratory of Urban and Regional Ecology, Research Center for Eco-Environmental Sciences, Chinese Academy of Sciences, Beijing, China.
[4]Faculty of Environment, University of Waterloo, Waterloo, Ontario, Canada.

Corresponding author: M. Leite Ribeiro, Laboratory of Hydraulic Constructions, Ecole Polytechnique Fédérale de Lausanne, Station 18, XX Lausanne, Switzerland. (mleiteribeiro@stucky.ch)

0043-1397/12/2011WR011296

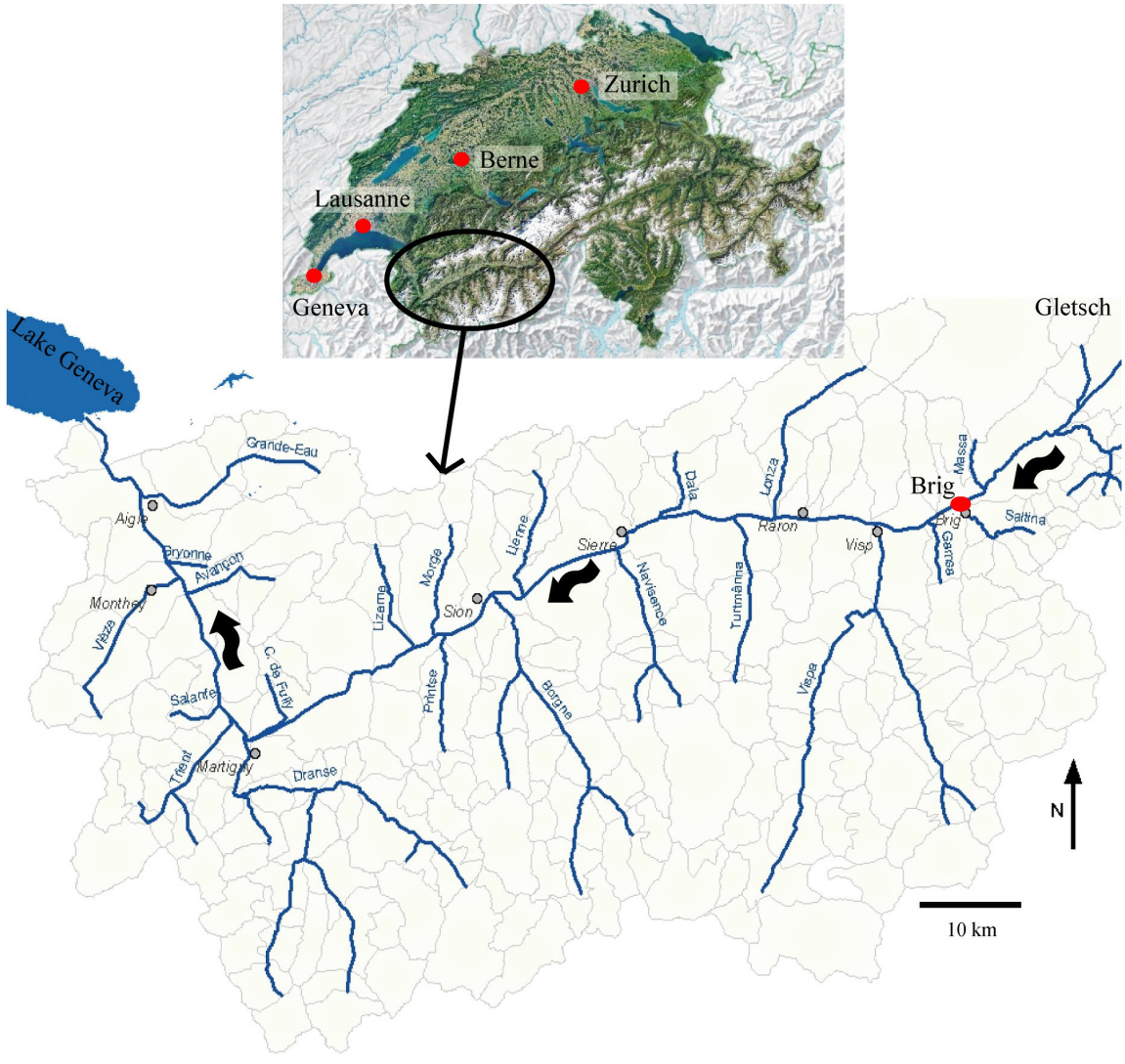

Figure 1. Upper Rhone River basin showing the twenty main confluences between Brig (upstream at the right in the figure) and Lake Geneva (downstream, at the left in the figure).

heterogeneity and fragmentation of the river system have been severely affected by these engineering interventions, which are believed to be an important cause of ecological degradation [*Fette et al.*, 2007; *Peter et al.*, 2005]. At present, a major river rehabilitation project is in progress in the Upper Rhone basin with the aim of achieving both improved flood protection and enhanced ecological value [*Weber*, 2006]. The rehabilitation of confluences with the aim to locally increase heterogeneity, improve habitat and enhance longitudinal connectivity, is an important component of the overall rehabilitation project. The design of the confluence rehabilitation is, however, hindered by a lack of understanding of the relevant hydromorphosedimentary processes and their interactions with ecological processes at these sites.

[6] Fluvial processes at confluences are known to depend on the planform and slope of the confluent channels, confluence angle, discharge and momentum flux ratios, bed material and sediment supply. *Leite Ribeiro et al.* [2012] have summarized and examined the foregoing investigations of [*Best*, 1988; *Biron et al.*, 1993; *Boyer et al.*, 2006; *Leclair and Roy*, 1997; *Rhoads and Kenworthy*, 1995; *Rhoads et al.*, 2009] on hydromorphosedimentary processes within what *Kenworthy and Rhoads* [1995] have referred to as the confluence hydrodynamic zone (CHZ)—the zone within, upstream and downstream of the confluence affected by flow convergence. *Leite Ribeiro et al.* [2012] have concluded that the current understanding is based on a surprisingly small number of investigated configurations, as represented by the conceptual models of *Best* [1988] based on laboratory experiments, *Leclair and Roy* [1997] and *Boyer et al.* [2006] based on investigations of the Bayonne-Berthier confluence and *Rhoads et al.* [2009] based on investigations of the confluence of the Kaskaskia River and Copper Slough. Due to considerably different confluence characteristics, none of these conceptual models can represent completely the hydromorphosedimentary processes in confluences on the Upper Rhone River. Based on detailed measurements of the morphology, the sediment size, the sediment transport, and the three-dimensional flow field in a laboratory flume in equilibrium conditions,

Leite Ribeiro et al. [2012] have proposed a conceptual model for confluences such as those on the Upper Rhone River, which have the following characteristics:

[7] The main channel provides the dominant discharge, as quantified by the discharge ratio Q_t/Q_m and momentum flux ratio $Mr = \rho Q_t U_t / \rho Q_m U_m$. Q is the discharge ($m^3\ s^{-1}$), ρ is the water density ($kg\ m^{-3}$), U is the mean velocity ($m\ s^{-1}$) and the subscripts t and m represent the tributary and main channels, respectively.

[8] 1. The sediment is predominantly and abundantly supplied by the tributary, and consists of poorly-sorted gravel with a high gradation coefficient.

[9] 2. The relatively steep tributary is smaller than the low-gradient main channel. The flow in the tributary is transcritical during formative floods, i.e., the Froude number is close to unity.

[10] Because this model, illustrated in Figure 2, serves as reference in the present investigation on tributary widening, its main features are briefly described. The pronounced bed discordance (*M1*) at the confluence mouth is due to the important difference between the flow depths in the steep tributary and in the low-gradient main channel. The formation of a stagnation zone (*F4*) at the upstream confluence corner causes an asymmetric distribution of the flow and sediment transport, whereby the sediment transfer between the tributary and the main channel mainly occurs near the downstream corner of the confluence. The presence of a large bar at the inner bank (*M2*) and the absence of a marked scour hole at the outer bank (*M5*) are typical of confluences characterized by a dominant and abundant sediment supply originating from the tributary and by low discharge and momentum flux ratios. The bar leads to a reduction in cross-sectional area and a corresponding acceleration of the flow that provides an increase in sediment transport capacity, which allows the load from the tributary to be transported through the CHZ. The pronounced bed discordance leads to the formation of a two-layer flow structure (*F1*, *F2*, *F3*). Flow originating from the tributary is mainly confined to the upper part of the water column of the main channel, where it deflects flow in the main channel outward. The bed discordance shields the flow in the lower part of the water column from the effects of the tributary inflow, allowing this flow to move unimpeded through the confluence and into the downstream channel. The two-layer flow structure does not lead

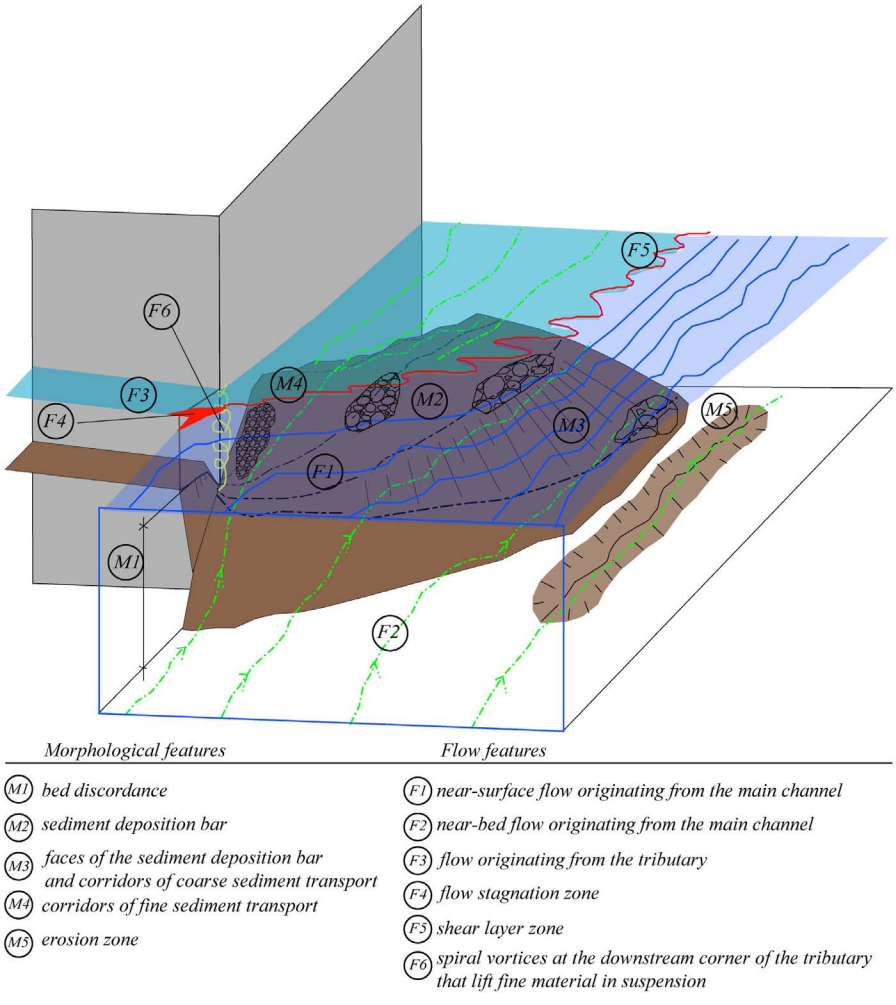

Figure 2. Conceptual model for hydromorphosedimentary processes in confluences between a small steep tributary with dominant supply of poorly sorted sediment and a larger low-gradient main channel with dominant flow supply [*Leite Ribeiro et al.*, 2012].

to the formation of secondary circulation cells. The near-bed flow originating from the main channel encounters at the confluence mouth coarse sediment supplied by the tributary. This near-bed flow moves over the sloping face of the bar (*M3*). It accelerates and has a component that is directed up the bar face. This component of the flow equilibrates the downslope gravitational force on the sediment particles and thereby conditions the slope of the bar face and the sediment sorting occurring on it. A shear layer (*F5*) develops where flows originating from the tributary and from the main channel collide. It is characterized by increased turbulence and its outer limit coincides closely with the toe of the bar (*M2*). In the downstream confluence corner, spiral vortices (*F6*) lift fine material into suspension. Fine materials are then transported near the inner bank (*M4*) while coarse sediments are transported on the bar face (*M3*).

[11] This paper reports on an investigation in a laboratory setting that is representative of the 20 major confluences on the Upper Rhone River. Specific aims of the investigation are to (1) analyze the hydromorphosedimentary implications of tributary widening through a comparison with the nonwidened condition (sections 3 and 4), (2) assess the potential of local tributary widening in the framework of river rehabilitation (section 5), (3) provide detailed experimental data on the flow, turbulence, sediment transport and bed morphology in a reference nonwidened configuration (which is reported in more detail by *Leite Ribeiro et al.* [2012]) and a configuration with local tributary widening.

2. Experiment Descriptions

[12] A laboratory investigation was performed under geometric and hydraulic conditions that are representative of the 20 major confluences on the Upper Rhone River. Table 1 summarizes the characteristics of these 20 confluences, as well as the variability in the principal parameters. The experimental set-up is not designed as a scale model of one particular confluence, but rather as a schematized configuration that aims at reproducing the dominant processes occurring in a broader range of configurations with the characteristics described in the introduction. The hydromorphosedimentary processes that occur in river confluences depend on numerous control variables and parameters, which cannot all be reproduced in laboratory models [*Yalin*, 1971; *Yalin and da Silva*, 2001] The experimental design primarily aims at reproducing the control variables and parameters that are expected to be of dominant importance, i.e., (1) the confluence geometry; (2) the flow characteristics; (3) the sediment characteristics.

[13] The confluence flume had smooth vertical banks and included a 8.5 m long and 0.50 m wide main channel. A 4.9 m long and 0.15 m wide tributary, connected at an angle of 90° entered the main channel at a distance of 3.60 m downstream of its inlet (Figure 3). The ratios of the tributary width to the main channel width of $B_t/B_m = 0.3$ and of the main channel width to the postconfluence channel width of $B_m/B_{p\text{-}c} = 1$ were typical of river channel confluences on the Upper Rhone River (Table 1). The intersection angles of the tributaries with the upper Rhone River are highly variable (Table 1). At present, these confluence angles are engineered rather than the result of natural morphodynamic processes. A local widening of the tributary may lead to a morphodynamic adjustment of the confluence angle. For the present project, the maximum observed value of 90° has been adopted in the nonwidened reference configuration. In the experiment reported here, the width of the tributary was symmetrically doubled ($B_w = 0.30$ m), over a distance from the tributary channel mouth that is three times the reference tributary channel width ($L_w = 3^*B_t = 0.45$ m). Figure 3 shows the experimental set-up including the geometry of the locally widened tributary channel and the reference configuration. An orthogonal (*X*, *Y*, *Z*) reference system was adopted for the experiments, where the *X*-axis is along the main channel in streamwise direction, the *Y*-axis points toward the left and has its origin at the right bank of the main channel (outer bank), and the *Z*-axis is vertically upward.

[14] The flow discharges of the main and tributary channels were $Q_m = 18.0\ \mathrm{l\ s^{-1}}$ and $Q_t = 2.0\ \mathrm{l\ s^{-1}}$, respectively, leading to a discharge ratio $Q_t/Q_m = 0.11$—a value typical for the Rhone basin under formative hydrological conditions corresponding to floods with return periods of approximately 2–5 years. In the reference configuration, this discharge ratio corresponds to a momentum flux ratio of $Mr = \rho Q U_t/\rho Q U_m = 0.20$, where ρ is the water density (kg m^{-3}) and U the mean velocity (m s^{-1}). Constant flow discharges were supplied by two independent pumps, connected upstream of the main channel and the tributary. An adjustable tailgate at the end of the main channel fixed the downstream flow depth at 0.07 m. Initial flow depths in the main channel and in the tributary were 0.09 m and 0.06 m, respectively.

[15] The movable bed was initially flat in the main channel and consisted of a sediment mixture characterized by $d_{50} = 0.82$ mm; $d_m = 2.3$ mm and $d_{90} = 5.7$ mm with a gradation coefficient $\sigma = 4.15$, where $\sigma = 0.5 * (d_{84}/d_{50} + d_{50}/d_{16})$. A constant sediment discharge of 0.30 kg min^{-1} from the same sediment mixture was supplied by a conveyor belt at the tributary inlet only. The sediment characteristics and the sediment discharge adopted for the experiments satisfied three requirements: (1) a longitudinal slope in the tributary in the range of those found in the

Table 1. Geometric and Hydraulic Characteristics of the Main Confluences on the Upper Rhone River[a]

	Angle (deg)	B_t/B_m	$B_m/B_{p\text{-}c}$	Tributary Bed Slope (%)	$Q2_t/Q2_m$	$Q5_t/Q5_m$	Fr_{tQ2}	Fr_{tQ5}	M_r_Q2	M_r_Q5
Average	62	0.22	1.02	1.1%	0.10	0.09	0.83	0.83	0.12	0.08
Max	90	0.54	1.27	4.0%	0.32	0.31	1.29	1.30	0.45	0.30
Min	30	0.07	0.71	0.0%	0.01	0.01	0.03	0.03	0.00	0.00

[a]*B* is the channel width, *Q*2 and *Q*5 are the discharges with a return period of 2 and 5 years, respectively, *Fr* is the Froude number, $Mr = \rho Q_t U_t/\rho Q_m U_m$ is the momentum flux ratio, where ρ is the water density and *U* the mean velocity, and the subscripts *t*, *m* and *p-c* represent the tributary, main channel and postconfluence channel, respectively.

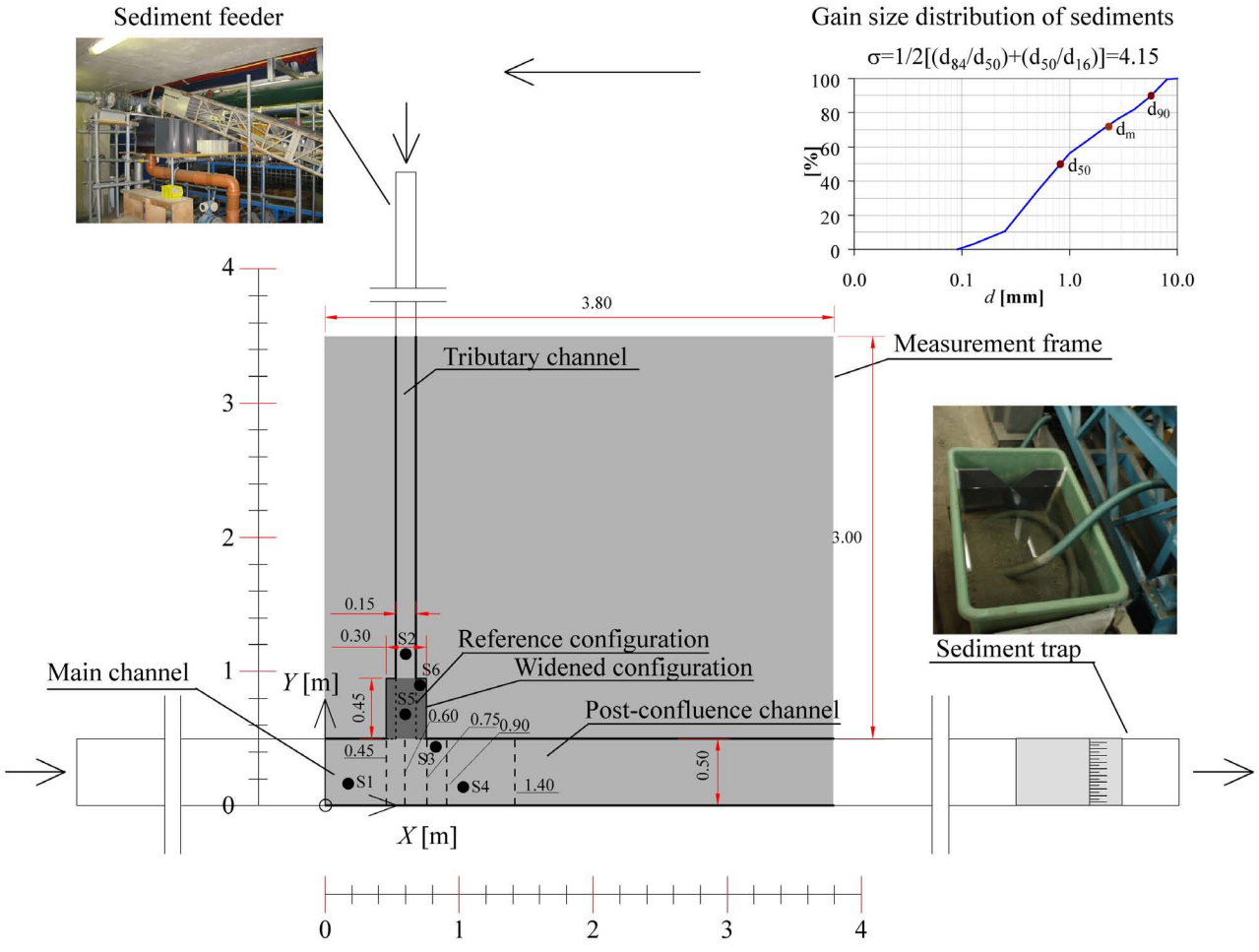

Figure 3. Experimental set-up, (X, Y, Z) reference system and grain size distribution of the supplied sediment. The cross sections where velocity measurements were performed are indicated by the dashed lines and the locations of the bed samples by the dark circles. The limit between the main channel and the postconfluence channel is the tributary axis at $X = 0.60$ m.

Upper Rhone (Table 1), (2) a Froude number in the tributary that is close to unity; (3) grain size sorting representative of the Upper Rhone within the reach that encompasses the 20 main considered confluences [*Leite Ribeiro*, 2011, Figure 3–16]. The normalized particle size distribution of the sediment is similar to those found in the Upper Rhone (Figure 4).

[16] The bed was initially covered with the poorly sorted sediment mixture in the main channel and the tributary. Before the beginning of the run, the bed was flattened in the main and postconfluence channels and had an initial longitudinal slope of around 0.05% in the tributary. The steady flow discharges were provided to the main channel and the tributary, respectively, and 0.3 kg min^{-1} of sediment was fed to the tributary only. This procedure aimed at reproducing conditions where the main channel's bed is armored and its banks are protected, and where floods in the steep tributary carry important loads of sediment. Such conditions are encountered in the Upper Rhone River. A sediment trap at the downstream end of the main channel

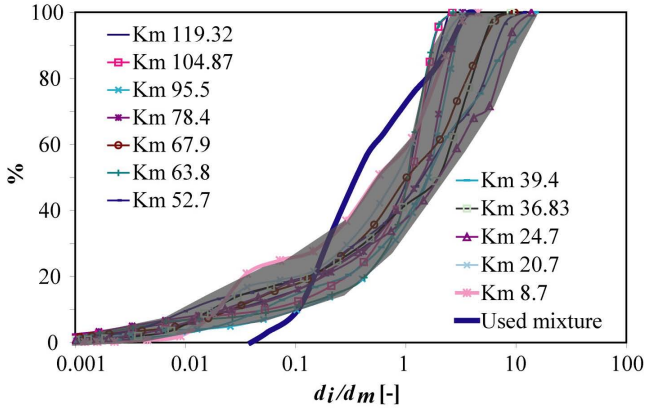

Figure 4. Distributions of the grain size normalized with the average grain diameter of the bed surface for the sediment mixture used in the laboratory experiments and for different locations on the Upper Rhone River (upstream distances with respect to Lake Geneva).

recovered the transported sediment. During the experiment, sediment volumes entering and leaving the flume were weighed. Equilibrium conditions, defined by a steady level of the bed topography and identical sediment fluxes entering and leaving the flume, were reached after 22 h in the configuration with local tributary widening and after 23 h in the reference configuration.

[17] Water surface elevations were measured with echo sounders for durations of 10 s at a frequency of 128 Hz, providing an average value with an accuracy of ± 1 mm. The bed topography was measured with a Mini Echo Sounder with an accuracy of ± 1 mm. Both instruments were installed on a movable frame that covers part of the experimental set-up (3.80 m in the main and postconfluence channels and 3.00 m in the tributary, see Figure 3). Table 2 summarizes information on the measuring grids for the widened test. The bed topography maps reported hereafter were obtained by bilinear interpolation between the measured points.

[18] Once the equilibrium bed morphology was established, nonintrusive measurements of velocity profiles were made with an Acoustic Doppler Velocity Profiler (ADVP) developed at École Polytechnique Fédérale Lausanne (Switzerland). The working principle of the ADVP has been described by *Lemmin and Rolland* [1997], *Hurther and Lemmin* [1998], *Blanckaert and Graf* [2001] and *Blanckaert and Lemmin* [2006]. *Blanckaert* [2010] described in detail the data treatment procedures and quantified the uncertainty in the measurements as follows: approximately 4% in the time-averaged longitudinal velocity u_x, approximately 10% in the cross-stream velocities (u_y, u_z), approximately 20% in the turbulent kinetic energy (*tke*). More details about the application of the ADVP in the confluence flume are reported in *Leite Ribeiro et al.* [2012]. Flow velocities were measured in five cross-sections in the main and postconfluence channels. The positions of the cross-sections were chosen to facilitate comparison between both configurations, i.e., the upstream corner of the confluence ($X = 0.53$ m and $X = 0.45$ m for the reference and widened configurations, respectively), the axis of the tributary ($X = 0.60$ m for both cases), the downstream corner of the confluence ($X = 0.68$ m and $X = 0.75$ m, respectively), a distance that corresponds to a tributary width (0.15 m) downstream of the confluence ($X = 0.83$ m and $X = 0.90$ m, respectively) and 0.65 m downstream ($X = 1.33$ m and $X = 1.4$ m, respectively) of the confluence.

[19] Samples of the surface bed material under equilibrium conditions were collected at different locations (Figure 3) and grain size analysis by sieving was performed. In the reference configuration, samples were collected in the main channel upstream of the confluence (S1), the tributary (S2), the top (S3) and the toe (S4) of the bar face. In the widened configuration additional samples were collected in the center (S5) and the downstream corner (S6) of the widened zone (Figure 3).

3. Water Surface Elevation, Bed Morphology, and Sediment Transport

[20] The main morphological features (Figure 5) in the configuration with the local tributary widening are similar to those schematized for the reference configuration in Figure 2, i.e., (1) the formation of a pronounced bed discordance between the tributary and the main channel; (2) the presence of a large bar downstream of the confluence at the inner bank; (3) slight scour near the outer bank (see also Figure 7e). The local tributary widening does, however, induce systematic morphological changes, as highlighted in Figure 6 for the tributary and in Figure 7 for the main and postconfluence channels.

[21] Water surface elevations in the widening are similar to those in the reference configuration (Figure 6). However, there is an overall increase in bed elevation in the local tributary widening compared to the reference configuration. The increase in the bed elevation is however, not constant and therefore the widened zone is characterized by a pronounced variability in flow depths (Figure 6). The flow depth along the axis of the channel is reduced to approximately 0.01 m, which corresponds to approximately half of the flow depth in the reference configuration (Figure 6), and the flow depth in the thalweg (=0.018 m) is still less than in the reference configuration. The main-channel flow causes a deviation of the thalweg toward the inner (downstream) bank of the widened zone (Figures 6b and 6c). Moreover, it creates dry zones and zones of flow stagnation near the outer (upstream) bank (Figure 6b). Local widening of the tributary is associated with a reduction of approximately 15% in effective cross-sectional flow area measured at $Y = 0.55$ m as compared to the reference configuration. This reduction leads to an increase in the tributary velocities and a corresponding increase in the tributary momentum flux. The increase of the tributary flow velocity and the reduction of the tributary flow depth lead to an increase in the bed discordance height and a deeper penetration of the tributary flow into the main channel (Figure 6a, Figure 7a).

[22] The bed discordance is oblique with respect to the main channel and nearly perpendicular to the thalweg at the tributary mouth (Figure 5, Figure 7a). The local

Table 2. Measuring Grids for the Water Surface Elevation and the Bed Topography for the Widened Test

Location	Water Level	Bed Topography
Main channel and postconfluence channel	Three transverse points ($Y = 0.05$, $Y = 0.25$ and $Y = 0.45$ m) in nine cross-sections ($X = 0.03$, $X = 0.44$, $X = 0.50$, $X = 0.60$, $X = 0.72$, $X = 0.74$, $X = 1.18$, $X = 2.18$ and $X = 3.18$ m).	Thirteen longitudinal profiles (measuring grid of $\Delta X = 0.009$ m in the domain $X = 0$ to 3.80 m) spaced by $\Delta Y = 0.04$ m from $Y = 0.04$ to $Y = 0.46$ and additional profile at $Y = 0.48$ m.
Tributary upstream of the local widening	Eight points on the tributary axis spaced by $\Delta Y = 0.20$ m between $Y = 1.04$ and $Y = 3.44$ m.	Points on the tributary axis with a spaced by $\Delta Y = 0.20$ m between $Y = 1.13$ and $Y = 1.33$ m.
Local tributary widening	Three transverse points ($X = 0.50$, $X = 0.60$ and $X = 0.72$ m) in five cross-sections ($Y = 0.54$, $Y = 0.64$, $Y = 0.74$, $Y = 0.84$ and $Y = 0.90$ m).	Nine cross-sections (measuring grid of $\Delta X = 0.009$ m in the domain $X = 0.475$ to $X = 0.725$ m) spaced by $\Delta Y = 0.05$ m from $Y = 0.54$ to $Y = 0.84$ and additional profile at $Y = 0.90$ m.

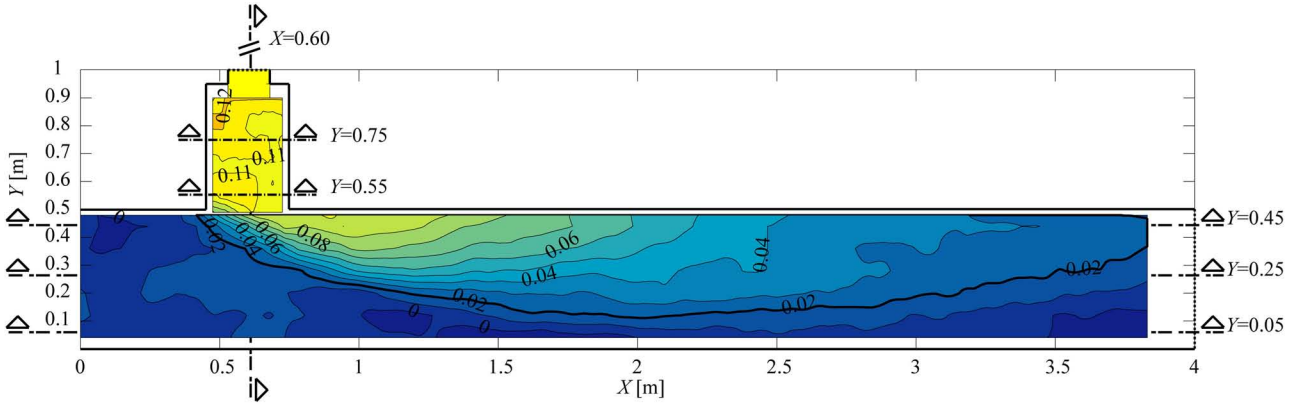

Figure 5. Equilibrium bed morphology for the main and postconfluence channels and the local tributary widening with indication of the two cross-sections in the tributary widening, the longitudinal profile along the tributary axis and the three longitudinal profiles in the main and postconfluence channels shown in Figure 6 and Figure 7. The reference level corresponds to the level of the initially horizontal bed and is situated at $Z = 0.02$ m (indicated by the thick black line).

tributary widening does not affect the average flow depth of approximately 0.02 m and the average bed slopes of approximately 1.9% in the tributary upstream of the widening. Moreover, the local tributary widening does not noticeably affect the water surface and bed elevations in the tributary upstream of the widening (Figure 6). Thus, local tributary widening does not modify hydraulic conditions in the tributary, an important consideration in flood safety.

[23] Figure 7 illustrates systematic morphological changes in the main and postconfluence channels induced by the local tributary widening. The increased discordance height and tributary penetration (Figure 6a) lead to a general rise in the bed level in the CHZ (Figure 7). Downstream of the tributary mouth, however, change in the cross-sectional averaged bed levels is small (Figure 7b) consisting merely of morphological redistribution (Figure 7a). This result is not unexpected because the flow and sediment discharge in the postconfluence channel are not modified by the local tributary widening. The morphological redistribution occurs by means of increased bed gradients. Increased deposition on the bar leads to the occurrence of a zone with an exposed channel bed at the inner bank just downstream of the confluence. This zone is approximately 0.65 m long (X-axis) and 0.08 m wide (Y-axis) and is covered by fine sand. The increased deposition at the inner bank is compensated by slightly increased scour near the outer bank (Figure 7e). The slope of the upstream face of the bar along the X-axis increases considerably from approximately 20% in the reference configuration

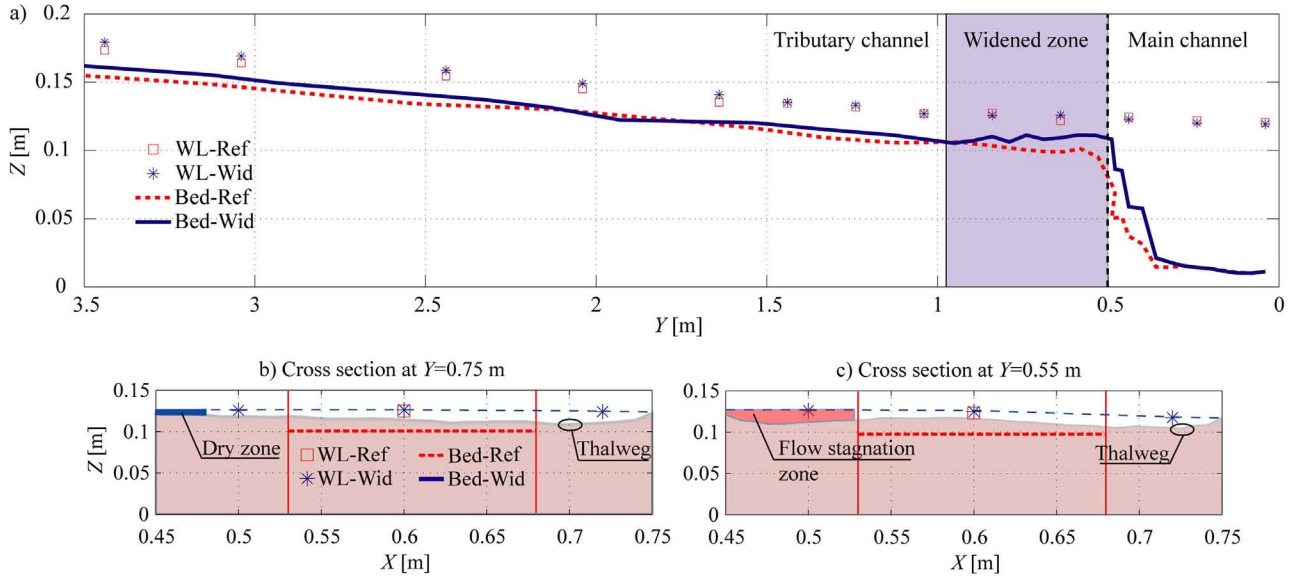

Figure 6. Comparison in the tributary of the water surface and bed elevations in the reference configuration and the configuration with local tributary widening. (a) Longitudinal profile along the axis of the tributary, (b and c) Cross-sections situated in the middle of the local tributary widening ($Y = 0.75$ m) and at the tributary mouth ($Y = 0.55$ m).

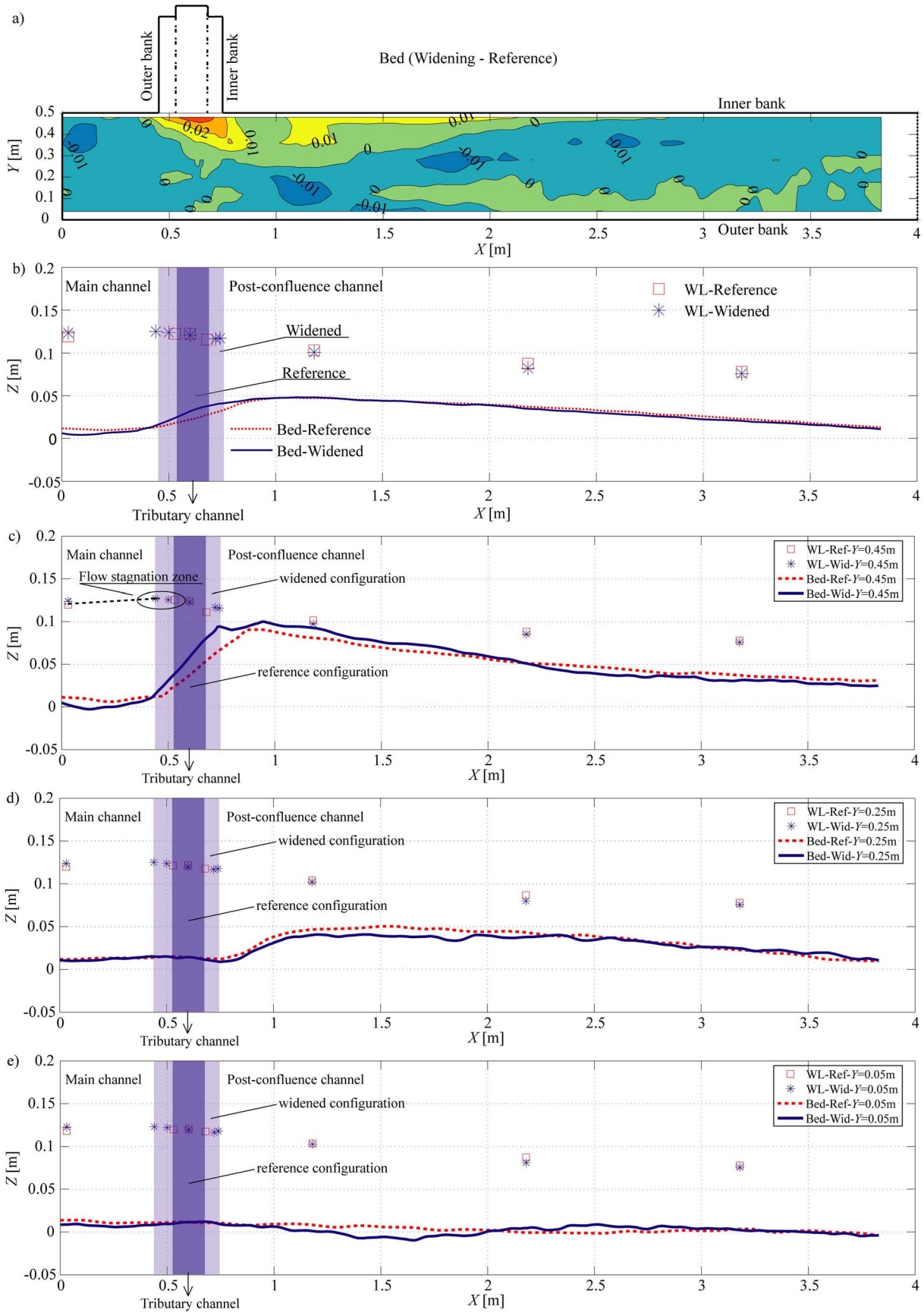
a)
Outer bank
Inner bank
Bed (Widening - Reference)
Inner bank
Outer bank
Y [m]
X [m]
b)
Main channel
Post-confluence channel
WL-Reference
WL-Widened
Widened
Reference
Bed-Reference
Bed-Widened
Tributary channel
Z [m]
X [m]
c)
Main channel
Post-confluence channel
Flow stagnation zone
widened configuration
reference configuration
WL-Ref-Y=0.45m
WL-Wid-Y=0.45m
Bed-Ref-Y=0.45m
Bed-Wid-Y=0.45m
Tributary channel
d)
Main channel
Post-confluence channel
widened configuration
reference configuration
WL-Ref-Y=0.25m
WL-Wid-Y=0.25m
Bed-Ref-Y=0.25m
Bed-Wid-Y=0.25m
Tributary channel
e)
Main channel
Post-confluence channel
widened configuration
reference configuration
WL-Ref-Y=0.05m
WL-Wid-Y=0.05m
Bed-Ref-Y=0.05m
Bed-Wid-Y=0.05m
Tributary channel

Figure 7

to approximately 27% in the configuration with local tributary widening (Figure 7c). The local tributary widening does not noticeably affect the water surface elevation in the main and postconfluence channels (Figures 7b–7e), suggesting that the local tributary widening does not have adverse effects on flood safety.

[24] Visual observations show that the sediment transport corridors in the local tributary widening also deviate toward the inner (downstream) bank (Figure 8a). In addition, two dry zones consisting of fine sediments form at the entrance of the local tributary widening. A third dry zone at the inner bank in the postconfluence channel shifts the flow and sediment transport corridors in the outward direction (Figure 8). As qualitatively indicated in Figure 8b, the sediment is mainly transported on the sloping bar face. The size of the transported sediment increases from the top to the toe of the bar face. This sediment sorting face is quantified by means of the grain size distributions in the sampling locations S3 and S4 on the top and near the toe of the bar face, respectively (Figure 9).

[25] Figure 9 compares the grain size distributions in corresponding locations in the reference and the local tributary widening configurations. The grain size distributions upstream of the CHZ in the main channel (*S1*) and upstream of the local tributary widening (*S2*) should not be affected by the local tributary widening. Differences between the grain size distributions in both configurations therefore give an indication of the uncertainty in the bed surface sampling procedure.

[26] The grain size distribution on the axis of the local tributary widening (*S5*) is considerably coarser than in the reference tributary (*S2*). This is consistent with the reduced effective flow area and increased velocities in the local tributary widening. The local tributary widening is characterized by a high heterogeneity in grain sizes, as indicated by the considerable differences in the grain size distributions in the locations S5 ($d_m = 5.4$ mm) and S6 ($d_m = 0.6$ mm).

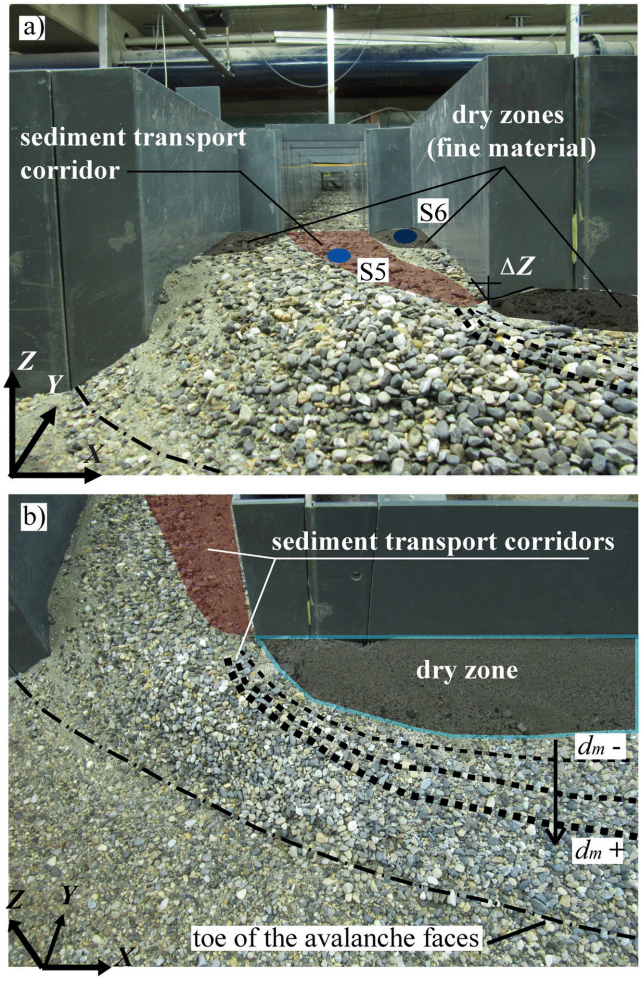

Figure 8. Sediment transport corridors, dry zones and face of the bar based on visual observations in the local tributary widening and the CHZ. The view is from the outer bank into the tributary. The thickness of the lines representing the sediment transport corridors indicates qualitatively the increase of the transported particle diameters.

4. Flow Dynamics

4.1. Flow Visualization

[27] Flow expands upon entering the local tributary widening (Figure 10). The influence of the flow in the main channel induces an asymmetry of this flow expansion, which is deflected toward the inner (downstream) bank of the widened zone. At a distance of 0.27 m from the entrance of the widened zone, the tributary flow reattaches to the inner (downstream) bank. The flow deflection, however, prevents the flow from reattaching to the outer (upstream) bank. As a result of this deflection, the tributary flow enters the main channel at an angle of approximately 65° (Figure 10).

[28] At the upstream corner of the confluence, flow originating from the main channel protrudes into the local tributary widening. The mutual backwater effect of the converging flows creates a zone of flow stagnation (Figure 10), which is characterized by a slight rise in the water surface elevation. This stagnation zone reduces the effective width of the tributary flow, which is not larger at the tributary mouth than in the reference configuration (Figure 10). The reduction in effective width and the reduced flow depth lead to increased tributary velocities and an increased tributary momentum flux into the main channel.

[29] The local tributary widening considerably modifies the flow field in the CHZ (Figure 11). The increased height of the bar leads to the formation of a dry zone at the inner bank just downstream of the confluence, which does not exist in the reference configuration. The dry zone has a length of approximately 0.65 m and a width of approximately 0.08 m. This dry zone and the increased tributary velocities shift the flow further toward the outer bank of the

Figure 7. Comparison in the main and postconfluence channels of the water surface and bed elevations in the reference configuration and the configuration with local tributary widening. (a) Differences in bed topography; (b) Longitudinal profile of the cross-sectional averaged water-surface and bed elevations; (c, d, and e) Longitudinal profiles near the inner bank ($Y = 0.45$ m), on the channel axis ($Y = 0.25$ m) and near the outer bank ($Y = 0.05$ m), respectively.

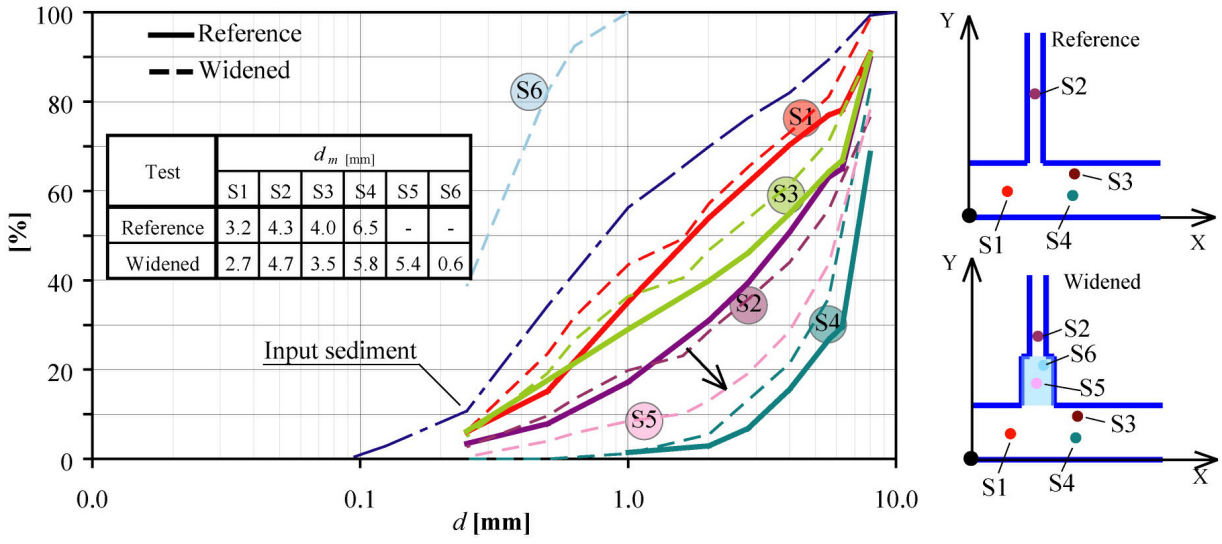

Figure 9. Grain size distributions in the sampled locations for the reference configuration (full lines) and the configuration with local tributary widening (dashed lines).

main channel as compared to the reference configuration. This shift is evident by comparing the positions of the shear layer generated by the collision of flow originating from the main channel and the tributary (Figure 11).

4.2. Depth-Averaged Flow Field

[30] Figure 12 shows the measured patterns of the unit discharges $(q_x, q_y) = (U_x h, U_y h)$ (h is the local flow depth) and the depth-averaged velocities (U_x, U_y) superimposed on a contour plot of the bed morphology in the CHZ for the configuration with local tributary widening. The local increase in depth-averaged velocity near the downstream corner of the confluence from $X = 0.60$ m to $X = 0.75$ m confirms the result of the flow visualization that the tributary flow is mainly conveyed into the main channel near the downstream corner of the confluence.

[31] The depth-averaged flow vectors are about parallel to the contour lines of the bed morphology, indicating the important role played by topographic steering: the flow steers around the highest areas and concentrates where bed morphology is lowest, which is in agreement with the requirements of mass conservation. This effect leads to considerable outward mass transport in the CHZ, accompanied by flow acceleration in the outer half of the cross-section and flow deceleration in the inner half of the cross-section. Downstream of the cross-section at $X = 1.2$ m (Figure 12), flow expansion leads to inward mass transport, as illustrated by the flow vectors measured in the cross-section at $X = 1.4$ m. The pronounced transverse variations in the flow depth h cause a pronounced nonuniformity of the unit discharge $U_x h$ over the width of the postconfluence channel.

[32] The local tributary widening leads to an amplification of the bed gradients (Figure 7a), which also amplifies the topographic steering of the flow. This amplification is illustrated in Figure 13, which assesses the influence of the local tributary widening on the bed morphology and the streamwise unit discharge by comparison of corresponding cross-sections in the reference configuration and the configuration with local tributary widening. The bed morphology

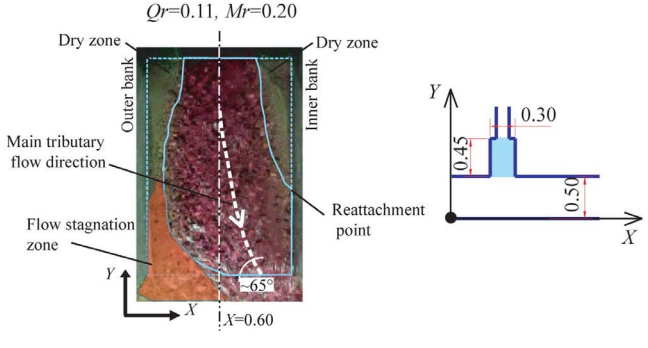

Figure 10. Flow visualization in the local tributary widening using color dye indicating the main flow features. The dashed rectangle in the left picture corresponds to the shaded area in the right picture.

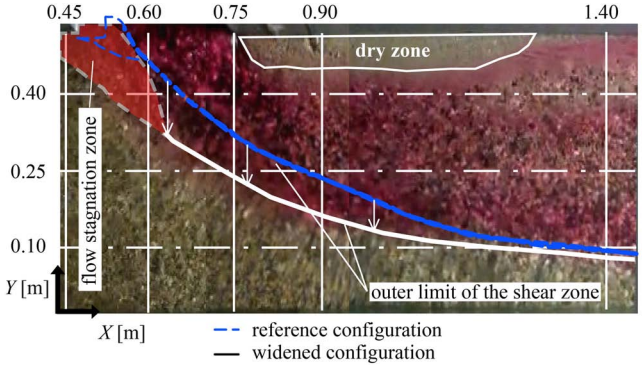

Figure 11. Flow visualization with color dye introduced in the tributary. Vertical white lines indicate the cross-sections where velocity measurements were performed. The location of the outer limit of the shear layers at the water surface is indicated by the full white line (configuration with local tributary widening) and by the dashed blue line (reference configuration).

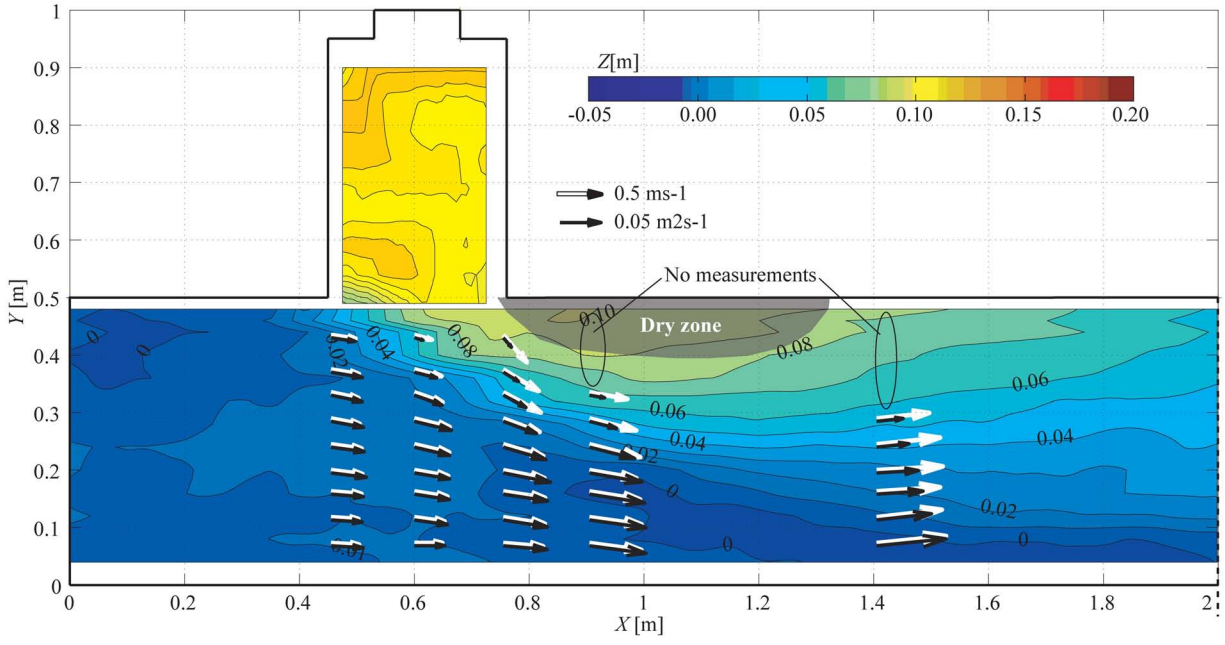

Figure 12. Contours of the bed morphology and vector representations of the depth-averaged unit discharges $(q_x, q_y) = (U_x h, U_y h)$ (full vectors) and the depth-averaged velocities (U_x, U_y) (dashed vectors). The dry zone is indicated by the shadow region.

and the unit discharge in the cross-section measured at the upstream corners of the confluence ($X = 0.53$ m and $X = 0.45$ m for the reference and widened configurations, respectively) are rather similar. The bed morphology and unit discharge already slightly increase in the outward direction, which is in agreement with the outward vectors observed in Figure 12. This skew can be attributed to topographic steering due to the presence of the bar as well as to the deflection by the inflow originating from the tributary.

[33] The local tributary widening has a marked influence on the bed morphology and the streamwise unit discharge from the cross-section located at the tributary axis. As

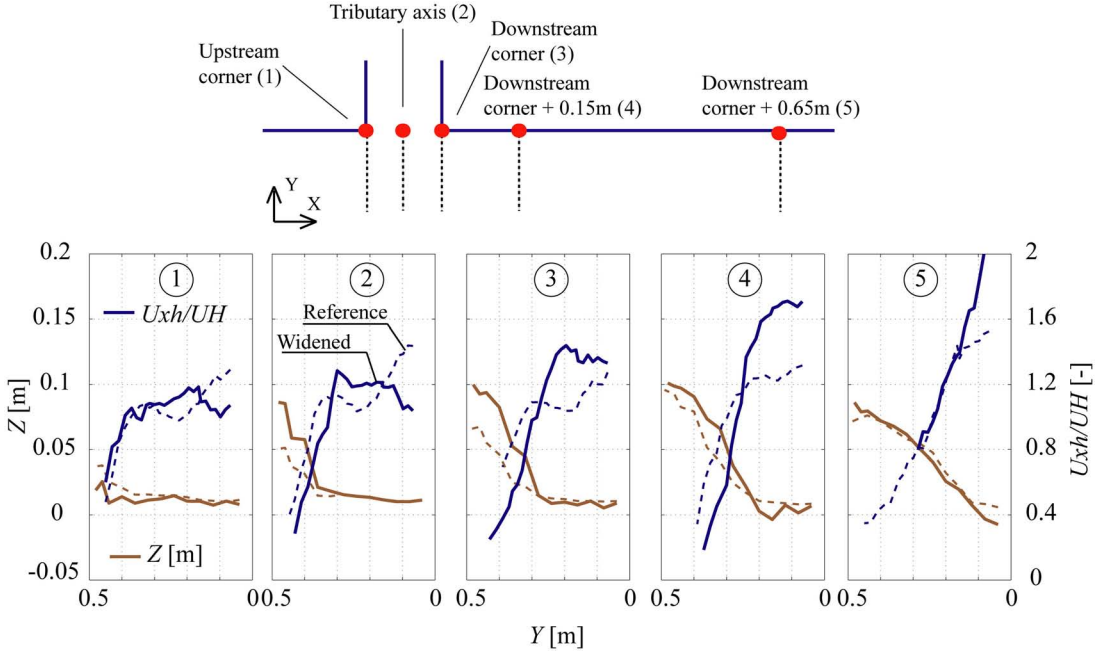

Figure 13. Comparison of the normalized streamwise specific discharge, $U_x h/UH$, and the bed morphology, in the reference configuration (dashed lines) and the configuration with local tributary widening (full lines). (1) At the upstream confluence corner; (2) At the tributary axis, (3) At the downstream confluence corner, (4) 0.15 downstream of the confluence, (5) 0.65 m downstream of the confluence.

illustrated in Figure 13, greater bar protrusion and bar development within and downstream of the confluence generally induces greater unit discharges near the outer bank and smaller unit discharges near the inner bank through topographic steering effects.

[34] The occurrence of a dry zone at the inner bank in the configuration with local tributary widening (Figure 11 and Figure 12) considerably affects the distribution of the unit discharge in the cross-section situated 0.15 m downstream of the confluence. It amplifies the decrease of the unit discharge in the inner part of the cross-section and leads to an increased unit discharge at the outer bank. Morphological differences between both configurations have diminished at the cross-section 0.65 m downstream of the confluence (Figure 7, Figure 13), which corresponds to the downstream limit of the dry zone in the configuration with local tributary widening (Figure 11). The unit discharge at the outer bank is still considerably higher, however, in the configuration with local tributary widening. Due to the increased scour (maximum approximately 0.015 m or approximately 15% of the flow depth) and the increased unit discharge near the outer bank, the local tributary widening may increase the flow attack on the outer bank.

4.3. Three-Dimensional Flow Field

[35] The local tributary widening does not fundamentally modify the hydrodynamic processes shown in Figure 2. The three-dimensional flow patterns in the CHZ in the configuration with local tributary widening are illustrated in Figure 14 by means of the patterns of the three mean velocity components (u_x,u_y,u_z) measured in five cross-sections along the main and postconfluence channels. The contour lines correspond to the streamwise velocities (u_x) whereas the vectors represent the transverse and vertical (u_y,u_z) velocities.

[36] The influence of the tributary is already discernable at the upstream corner of the confluence ($X = 0.45$ m) where considerable outward velocities occur. Different processes contribute to this transverse mass redistribution. The most important is probably topographic steering due to the presence of the bar that directs the flow outward. As shown by the flow visualization (Figure 11), the mutual backwater effects of the converging flows cause a stagnation zone which is characterized by a rise in the water level near the inner bank (Figure 10). These processes originate at the tributary mouth and weaken with distance from the inner bank.

[37] Flow from the tributary protrudes into the CHZ and postconfluence channel and thereby changes its direction in a zone approximately 1.5 m long (Figure 12). This tributary inflow mainly remains near the water surface, which is due to the pronounced bed discordance (Figure 6 and Figures 14b and 14c). This near-surface flow originating from the tributary occupies at maximum about two thirds of the width of the postconfluence channel (Figure 14d). A two-layer flow structure exists near the confluence mouth: flow in the upper part of the water column originating from the tributary is considerably more outward directed than flow in the lower part of the water column originating from the main channel. This effect is best discernible in the cross-sectional patterns of the transverse velocity (Figure 15a and 15c) and in the plan view of the horizontal velocity components near the bed and near the water surface (Figure 16a). This effect is most pronounced near the downstream corner of the confluence (Figures 14c, 15, and 16a) where the main tributary inflow occurs. The skewing of both flow layers does not lead to the generation of secondary flow cells.

[38] A shear layer is generated where both flow layers collide. Its position at the water surface was indicated by flow visualization in Figure 11. The three-dimensional shape of the shear layer is inferred from the cross-sectional pattern of the streamwise velocity (Figures 14b–14d), transverse velocity (Figure 15) and turbulent kinetic energy (*tke*) (Figure 17). Note that the indications provided by these different flow variables do not perfectly agree, whence the shear layer indicated in the figures does not perfectly coincide with the largest gradient in streamwise velocities (Figures 14b–14d) and the highest *tke* values (Figure 17). Note also that the shear layer is outside the measuring grid in the cross-section on the tributary axis ($X = 0.60$ m), and therefore only indicated in the figures for the cross-sections further downstream.

[39] The momentum input by the tributary increases the magnitude of the velocity vector near the inner bank (Figure 12, and compare Figure 14b and Figure 14c). The core of maximum streamwise velocities occurs in the lower part of the water column near the toe of the bar face (Figures 14b–14d). Its coincidence with the transport corridors of the coarsest sediment (Figure 8) indicates its importance with respect to sediment transport. In the cross-section situated at $X = 0.90$ m, i.e., 0.15 m downstream of the confluence (Figure 14d), the transverse velocities near the inner bank have weakened, but the two-layer flow structure and the core of highest velocities close to the bed near the inner bank are still discernible. This cross-section is characterized by an acceleration of the flow, especially on the slope of the bar near the inner bank. This flow acceleration, which plays an important role in the transport of sediment supplied by the tributary, can be attributed to three effects. First, the bar near the inner bank reaches its maximum height (Figure 5), which leads to a considerable reduction of the flow area. Second, the near-surface flow originating from the tributary occupies approximately two thirds of the width (see dye visualization in Figure 11) which leads to a contraction and further reduction of the area occupied by the flow originating from the main channel. Third, this reduction of the flow area is accompanied by

Figure 14. Mean streamwise flow velocities u_x (contourlines) and cross-sectional flow vectors (u_y, u_z) measured in the five cross-sections in the main and postconfluence channels indicated in Figure 3. The two vertical dashed lines represent the boundaries between measurements performed with different ADVP configurations, whereas the shaded areas indicate regions where the flow measurements are perturbed by the ADVP housing that touches the water surface (more information is provided in Leite Ribeiro *et al.* [2012]). The thick black line indicates the position of the shear layer as inferred from the velocity patterns (present figures), the patterns of the turbulent kinetic energy (Figure 17) and the flow visualization (Figure 11). The toe of the bar face is indicated by the gray ellipse.

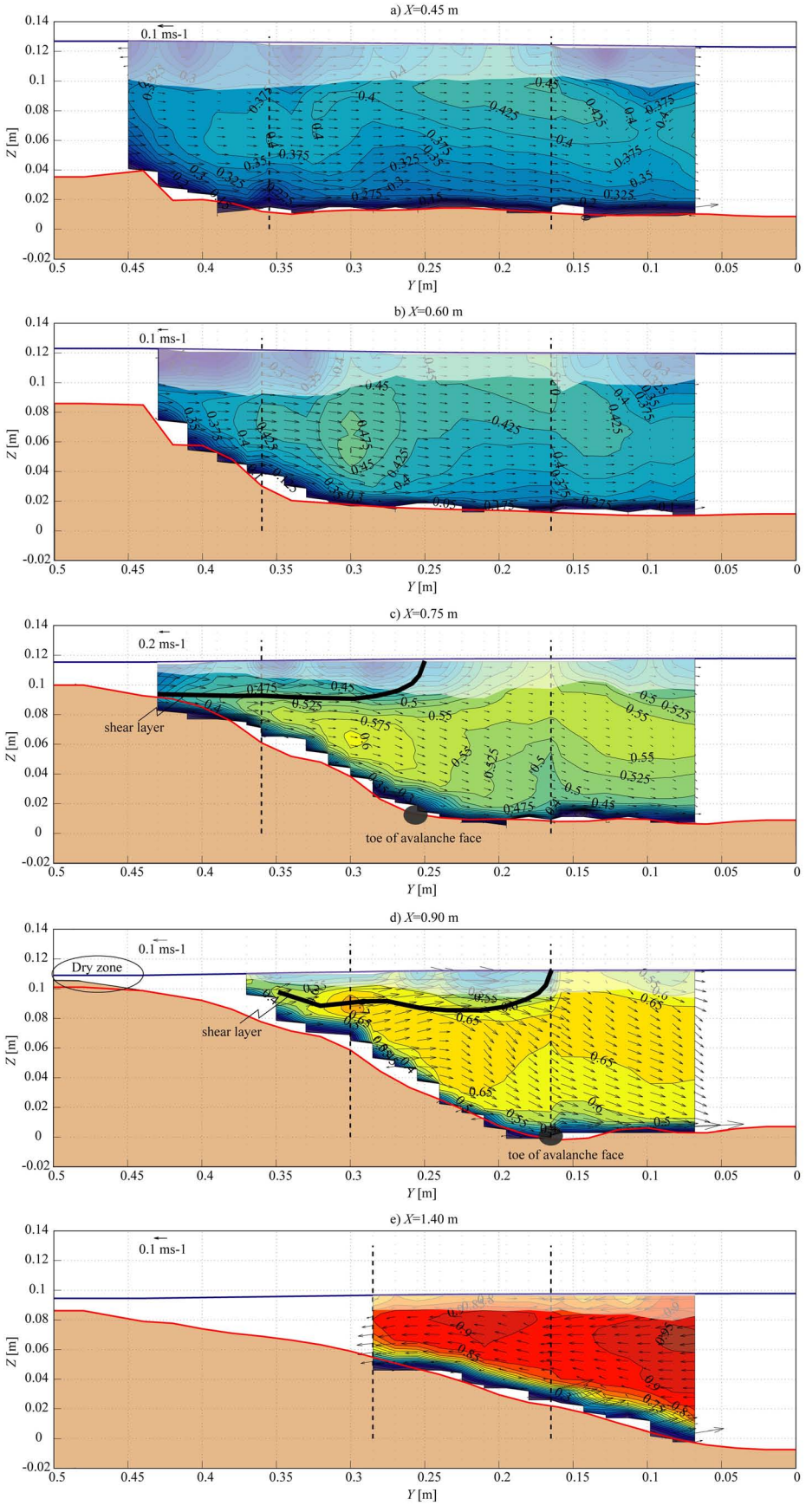
a) X=0.45 m
0.1 ms-1
b) X=0.60 m
0.1 ms-1
c) X=0.75 m
0.2 ms-1
shear layer
toe of avalanche face
d) X=0.90 m
0.1 ms-1
Dry zone
shear layer
toe of avalanche face
e) X=1.40 m
0.1 ms-1
Z [m]
Y [m]

Figure 14

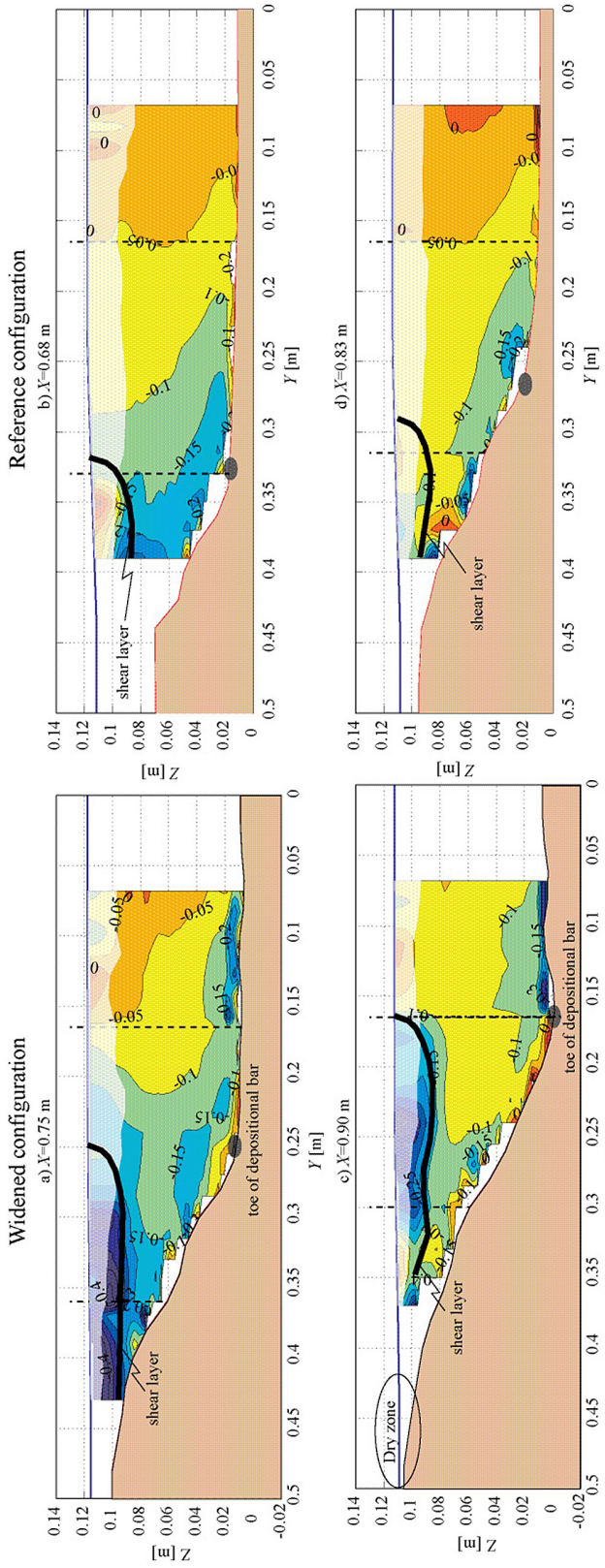

Figure 15. Comparison between the patterns of the transverse velocity, u_y, in the CHZ measured in the configuration with local tributary widening (left column) and the reference configuration (right column). The two vertical dashed lines represent the boundaries between measurements performed with different ADVP configurations, whereas the shaded areas indicate regions where the flow measurements are perturbed by the ADVP housing that touches the water surface (more information is provided in *Leite Ribeiro et al.* [2012]). The thick black line indicates the position of the shear layer as inferred from the velocity patterns (Figure 14), the patterns of the turbulent kinetic energy (Figure 17) and the flow visualization (Figure 11). The toe of the bar face is indicated by the gray ellipse.

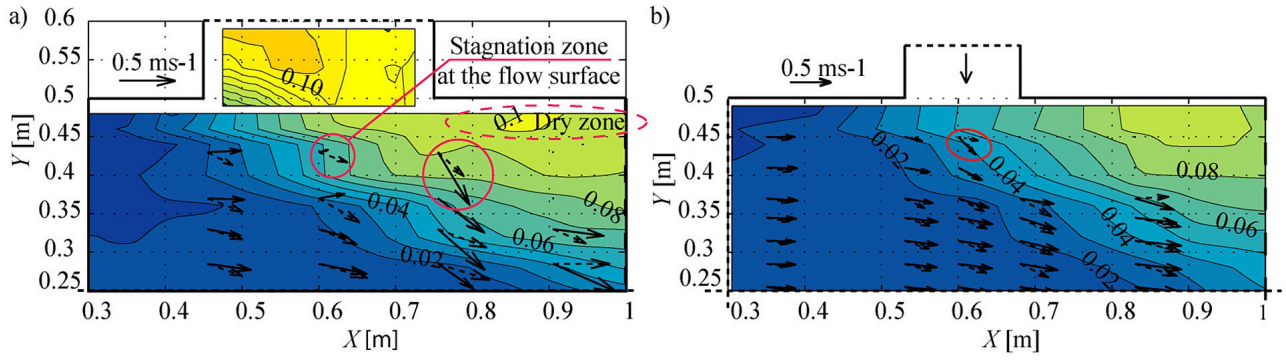

Figure 16. Velocity vectors (u_x, u_y) near the bed ($Z/h = 0.2$; dashed vectors) and near the surface ($Z/h = 0.7$, full vectors) superimposed on the local bed morphology; only the inner half of the width is shown. (a) configuration with local tributary widening, (b) reference configuration. The dashed circle in (a) indicates the dry zone.

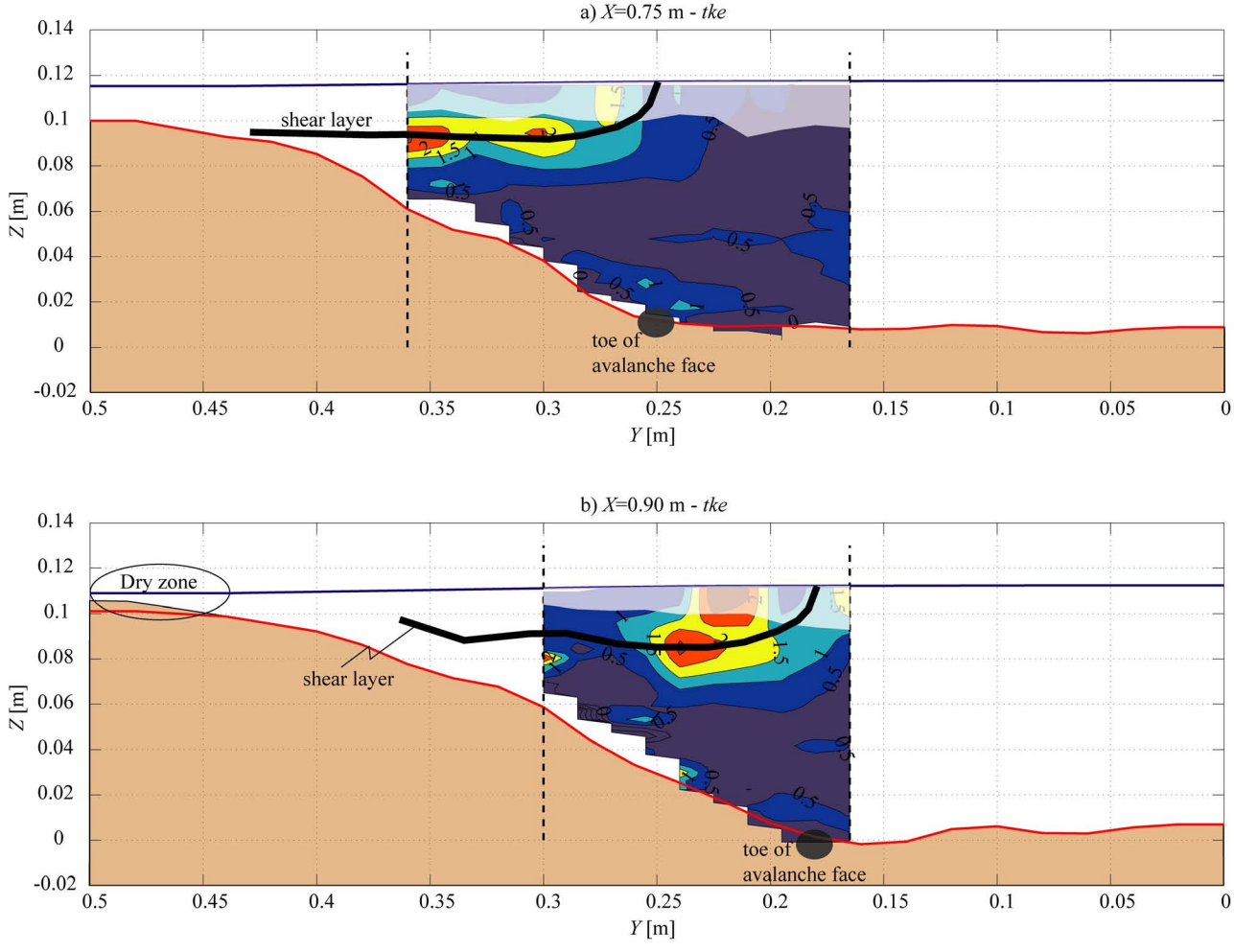

Figure 17. Patterns of the normalized turbulent kinetic energy (tke/u_*^2) in the cross-sections at (a) $X = 0.75$ m, (b) and $X = 0.90$ m in the configuration with local tributary widening. The characteristic shear velocity $u_* = 0.04$ ms^{-1} used for the normalization is the same as for the reference case [see *Leite Ribeiro et al.*, 2012].The shaded areas indicate regions where the flow measurements are perturbed by the ADVP housing that touches the water surface (more details in *Leite Ribeiro et al.* [2012]). The thick black line indicates the position of the shear layer as inferred from the velocity patterns (Figure 14), the patterns of the turbulent kinetic energy (present figure) and the flow visualization (Figure 11). The toe of the bar face is indicated by the gray ellipse.

a backwater effect that provides the local steepening of the water surface (Figure 7c) required to accelerate the flow.

[40] The 3-D flow patterns confirm the topographic steering of the flow which was identified in the depth-averaged flow patterns (Figure 12): flow goes outward over the entire flow depth in the inner half of the cross-section in regions where the bed elevation increases in streamwise direction (from the upstream corner of the confluence onto around $X = 1.1$ m according to Figure 5) and inward further downstream where the bed elevation decreases in streamwise direction (Figure 14e).

[41] The key element explaining the hydromorphosedimentary implications of the local tributary widening is the amplification of the tributary velocities (Figure 15). At the downstream corner of the confluence, where the dominant tributary inflow occurs (Figure 11 and Figure 12), the increased bed discordance and tributary penetration (Figure 6 and Figure 7) increase the transverse velocities (Figures 15a and 15b). Moreover, these transverse velocities penetrate further outward into the main channel. This increased transverse tributary input amplifies the two-layer flow structure and its delimiting shear layer generated by the collision of the flows originating from the tributary and the main channel. Non-negligible transverse velocities directed toward the outer bank occur close to the outer bank, and may enhance the flow attack on that bank. These differences induced by the local tributary widening persist in the cross-section 0.15 m downstream of the tributary widening (Figures 15c and 15d).

[42] That the hydrodynamic processes change in the confluence with local tributary widening is clearly illustrated in Figure 16, which compares the near bed ($Z/h = 0.2$) and near-surface ($Z/h = 0.7$) velocities in both configurations. Near the inner bank, the near-bed flow from the main channel follows a rather straight path and it has a component that is directed up the slope of the bar (most left near-bed vectors in $X = 0.60$ m. This upslope flow component conditions the slope of the bar face. The dominant tributary inflow (in $X = 0.75$ m in the widened configuration and in $X = 0.60$ m in the reference configuration) can easily be recognized by the near surface velocities that are outward directed. The local tributary widening considerably enhances the magnitude of these near-surface velocities as well as their outward direction. The skewing of these near-surface velocities with respect to the near-bed velocities illustrates the two-layer flow structure. The two-layer structure mainly occurs in the region confined by the shear layer, which coincides closely with the toe of the bar face. This region is considerably wider in the configuration with local tributary widening than in the reference configuration (Figure 15 and Figure 16). The presence of the stagnation zone where the tributary and main-channel flows collide is clearly discernable in the low near surface velocities, occurring near the tributary axis in the widened configuration and near the upstream confluence corner in the reference configuration (Figure 16).

4.4. Turbulent Flow Structure

[43] Confluences locally enhance the turbulence activity, which is relevant with respect to the mixing of mass, momentum, heat, suspended matter and the transport of sediment coming from the main channel and the tributary. The patterns of the normalized *tke* measured in the configuration with local tributary widening are displayed in Figure 17 for the cross-sections at the downstream corner of the confluence ($X = 0.75$ m) and 0.15 m downstream of the confluence ($X = 0.90$ m). Turbulence measurements were only performed in the central part of the cross-section as explained in *Leite Ribeiro et al.* [2012].

[44] The most noticeable features are the zones of pronounced *tke* increase. They occur in the upper part of the water column inside the shear layer and further accentuate the two-layer flow structure in the CHZ. The increased turbulence activity may be attributed to two processes. First the collision of the flows originating from the main channel and the tributary creates a shear layer (indicated in Figure 17) that is characterized by increased turbulence activity. Second, the momentum input by the tributary flow increases the magnitude of the velocities in the CHZ (Figure 12 and Figure 16) and hence also the turbulence activity, since *tke* scales with the square of the mean velocity magnitude. The tributary flow appears to be similar to a jet, and generates patterns of increased turbulence similar to a jet at the jet margins [*Rhoads and Massey*, 2012]. In line with observations in the reference configuration *Leite Ribeiro et al.* [2012], the core of pronounced *tke* increase in the shear layer about coincides with the preferential corridors of sediment transport (Figure 8).

5. Local Tributary Widening for River Rehabilitation

[45] At present, the main channel of the Upper Rhone is channelized at almost constant embanked width. The ecological state of the main channel is poor due to the spatially quasi-homogeneous flow and morphologic conditions. Most of the Upper Rhone's tributaries are also channelized and embanked immediately upstream of their confluences with the Rhone, but are in a better ecological state farther upstream [*Weber*, 2006]. Weirs or block ramps, constructed at the confluence mouth to stabilize the bed discordance, reduce the lateral connectivity as compared to natural bed discordant morphologies. This reduced connectivity is particularly severe during low flow stages. Confluence rehabilitation by local tributary widening may not only improve the local habitat heterogeneity in the main channel, but more importantly make the tributaries act as "sources" or "refugia" for biodiversity by improving their connectivity to the main channel system and by improving the local habitat in the widening.

[46] The improved connectivity plays a role not only locally, but for the whole river system. Connectivity is crucial for linking biological communities and populations within a catchment, maintaining genetic and taxonomic diversity and linking habitats for different life stages of aquatic organisms [*Lake et al.*, 2007; *Palmer*, 2009; *Rice et al.*, 2008]. The potential connectivity benefits of local tributary widenings on the Upper Rhone can be illustrated by considering the case of the lake resident brown trout (*Salmo trutta lacustris*), which has been investigated by *Champigneulle et al.* [1991] and Association Truite Léman (Reconstitution de zones propices à la reproduction naturelle des truites, available online at www.truiteleman.ch/dossier/publicationsf.htm, in french). The lake resident brown trout spawns in the Upper Rhone's tributaries. Juveniles remain in the tributaries for 1 to 2 years, and

subsequently migrate downstream to Lake Geneva (Figure 1). During their adult life, they migrate upstream from Lake Geneva to their spawning grounds in the period October–December, which generally coincides with a period of low flows. The spawning areas are vulnerable to floods during the winter and spring season. The lake resident brown trout is an endangered species in Switzerland: during the period 1986–1996, its presence decreased by 42% [*Friedl*, 1999]. Confluence rehabilitation by local tributary widening may improve connectivity for brown trout in two ways. First, the insight provided by our experiments into the formative mechanisms of the bed discordance should allow for a design of confluence mouths without hard engineering structures, such as weirs or block ramps. Such an improved design would allow organisms to migrate with fewer barriers between the main river and the tributaries, especially at low flows. Second, the increased heterogeneity of flow depths and velocities in the engineered section may provide additional spawning grounds, refugia during floods and overwintering habitats.

[47] In general, local tributary-mouth widening may locally enhance habitat for a broad range of aquatic biota. The main flow corridor has coarse material at the bed surface, active sediment transport, high flow depths and high velocities. The additional dry zones and flow stagnation zones, introduced by the engineered widening, have fine material at the bed surface and low flow velocities. Bed surface material, flow depth and velocities also show variability within each of these flow regions. Bed surface material, flow depth and velocities are known to be dominant control parameters for aquatic biota (e.g., macroinvertebrates, fishes and vegetation), and they are key parameters in habitat suitability models [*Schweizer et al.*, 2007b]. The increased heterogeneity in these dominant control parameters could offer an appropriate habitat for a much wider range of biota than the homogeneous, channelized reference configurations.

[48] The natural temporal variability in flow discharge and sediment load are important for biota [*Palmer et al.*, 1997] and can be expected to further increase the system's heterogeneity by causing temporal variations in the location and size of the tributary main flow corridor, dry zones and flow stagnation zones. Moreover, temporal variability is essential for remobilizing bed substrate and supplying organic matter. The dry zones identified in the reported laboratory experiments under bed-forming conditions can be expected to be dry during low discharges and inundated with relatively weak flow during flood conditions. They could be a suitable habitat for the development of a riparian ecosystem, including vegetation colonization of exposed bar surfaces [*Schweizer et al.*, 2007a; *Singer and Dunne*, 2006; *Weber et al.*, 2009], and could form an essential connection between aquatic and terrestrial ecosystems. The flow stagnation zones are characterized by weak flow conditions, and can therefore be expected to play an important role as refugia for aquatic biota during flood events.

[49] It is clear, however, that the quasi-homogeneous hydrodynamic and morphologic conditions in the engineered confluence are only one of the limiting ecological factors in the Upper Rhone river network. Creating an appropriate physical habitat through tributary widening does remove an important limiting factor, but cannot guarantee on its own ecological improvement. The ecological improvement requires the establishment of a biological community including essential linkages between different species and their dependency on physical quantities. The lake resident brown trout, for example, requires a sufficient physical-chemical water quality during its reproduction stage. Emergent and riparian vegetation also play an important role: they favor the development of macroinvertebrate communities which are at the basis of the juvenile trout's food web, and they provide shelter zones for juvenile and adult trout and other fish species. We refer to *Palmer et al.* [1997] and *Lancaster and Downs* [2010] for a detailed discussion of the role of habitat restoration in the reestablishment of species and ecological function.

[50] The local widening of the tributary for rehabilitation purposes is only acceptable if it does not induce adverse impacts on flood safety. In the laboratory experiments reported here and in 10 additional experiments of *Leite Ribeiro* [2011], the local widening did not noticeably affect the water surface elevations in the tributary upstream of the widening (Figure 6) and in the postconfluence channel (Figures 7b–7e). This suggests that the local tributary widening does not have adverse impacts on flood safety for inbank flows, although it might enhance the flow attack on the main channel's outer bank just downstream of the confluence, which may need to be accommodated in rehabilitation schemes. But the laboratory experiments only considered steady state equilibrium configurations for a limited number of discharge scenarios. Further experiments are required for simulating the dynamic evolution of the bed and water surface topographies during flood events to preclude any increased flood risk.

[51] The experimental set-up was designed as a schematized configuration based on the control parameters for the geometry, the flow and the sediment that were expected to be of dominant importance. The experimental design aimed at reproducing the dominant processes occurring in a broader range of configurations characterized by relatively low discharge and momentum flux ratios where small steep tributaries with a high supply of poorly sorted sediment join a low-gradient stream. *Leite Ribeiro et al.* [2012] have shown that the reference experiment without tributary widening reproduced satisfactorily the main features observed in the Upper Rhone confluences, which lends credibility to the results of the laboratory investigation. Obviously, the details of the hydrodynamic and morphologic patterns will depend on numerous parameters, including the configuration of the engineered confluence, the geometry of the tributary widening, the discharge and sediment transport scenarios and the sediment characteristics. *Leite Ribeiro* [2011] has investigated the effect of the discharge scenario and the geometry of the local tributary widening in a series of 12 experiments in the same experimental set-up: three different discharge scenarios in the reference nonwidened configuration and in three different geometries of the local tributary widening. Detailed measurements of the flow and turbulence were only obtained in the two experiments reported in the present paper, whereas the other experiments focused on the morphology. The analysis confirmed the reproducibility and the robustness of the main results, which are the enhanced processes in the CHZ, and especially the increased heterogeneity and complexity of the flow, morphology and sediment in the local tributary widening. For all experiments, the flow depth in the widening

was very heterogeneous with deep zones, shallow zones and even the appearance of dry zones. The flow field included corridors of high velocities corresponding to the corridors of sediment transport, zones of weak velocity and recirculation zones. The sediment ranged from the coarsest material in the high-velocity corridors of sediment transport to the fines material in the recirculation zones and the dry zones. Local tributary widening can reasonably be expected to provide enhanced hydraulic habitat without adversely affecting flooding in a wide range of confluence configurations. The result of the present laboratory investigation cannot, however, straight forwardly be extrapolated to field confluences, or to confluences with characteristics that differ from those investigated.

6. Conclusions

[52] Channelized fluvial systems are characterized by a reduced heterogeneity in flow, sediment and morphology characteristics, which contributes to the impoverishment of fluvial ecosystems. The hydromorphological implications and the ecological potential of a local tributary widening were investigated in a laboratory setting that is representative of the 20 major confluences on the Upper Rhone River, Switzerland.

[53] The local tributary widening considerably affects the hydromorphosedimentary processes in the confluence hydrodynamic zone (CHZ). Although the local tributary widening reduces the angle of entry of the tributary flow, it leads to an amplification of the hydromorphosedimentary processes in the CHZ with respect to the reference configuration. This result is due to the reduction of the effective flow area in the local tributary widening and the corresponding increase in the tributary velocities and the tributary momentum flux. The reduction in effective flow area is necessary to satisfy the requirement for sediment transport continuity in the local tributary widening. It occurs by means of a general rise in the bed elevation and by a lateral constriction of the flow induced by a zone of flow stagnation at the upstream confluence corner. The increased tributary velocities accentuate and amplify a two-layer flow structure in the CHZ. Flow originating from the tributary remains in the upper part of the water column and is strongly outward directed while flow originating from the main channel remains in the lower part of the water column and is considerably less outward directed. This two-layer flow structure does not, however, generate secondary flow cells. A pronounced shear layer characterized by increased turbulence activity develops at the interface between flows originating from the main channel and the tributary. The increased tributary momentum flux due to local tributary widening leads to a more pronounced bed discordance and to enhanced penetration of the tributary flow into the CHZ for the studied discharge scenario. Downstream of the CHZ, higher deposition in the inner part and scour in the outer part of the cross-section amplify the bed morphology gradients. This morphological effect amplifies topographic steering of the flow and the corresponding transverse fluxes of mass and momentum.

[54] In the physical model runs the heterogeneity of the sediment substrate, the flow velocities and the flow depths is significantly increased by the local tributary widening, which suggests that in rivers, tributary widening has the potential to enhance habitats. Furthermore, such a local tributary widening can improve the connectivity of the tributary to the river network, and thus local confluence interventions might have system-wide ecological benefits. In the investigated configurations, the local tributary widening does not have adverse effects on flood safety, neither in the tributary upstream of the local widening, nor in the post-confluence channel, although it could enhance the flow attack on the outer bank in the postconfluence channel.

[55] Local tributary widening can reasonably be expected to provide enhanced hydraulic habitat without adversely affecting flooding in a wide range of confluence configurations. But no ecological data is yet available to confirm these ecological benefits, and no hydromorphological data is yet available from field confluences. The result of the present laboratory investigation cannot straight forwardly be extrapolated to field confluences, or to confluences with characteristics that differ from the investigated ones. The reported results merely support the implementation of this rehabilitation strategy of local tributary widening by direct engineering intervention.

[56] **Acknowledgments.** The research was supported by the Swiss Federal Office for the Environment (FOEN) in the framework of the project "Integrated management of river systems." The second author was partially supported by the Chinese Academy of Sciences Visiting Professorship for Senior International Scientists, grant 2011T2Z24, by the Sino-Swiss Science and Technology Cooperation for the Institutional Partnership Project, grant number IP13_092911. The paper was considerably improved thanks to input by Armin Peter, leader of the group Restoration Ecology at EAWAG, in Switzerland and by the reviewers, Bruce Rhoads and Stephen Rice.

References

Benda, L., N. L. Poff, D. Miller, T. Dunne, G. Reeves, G. Pess, and M. Pollock (2004), The network dynamics hypothesis: How channel networks structure riverine habitats, *BioScience*, *54*, 413–427.

Best, J. L. (1988), Sediment transport and bed morphology at river channel confluences, *Sedimentology*, *35*, 481–498.

Biron, P., A. G. Roy, J. L. Best, and C. J. Boyer (1993), Bed morphology and sedimentology at the confluence of unequal depth channels, *Geomorphology*, *8*, 115–129.

Blanckaert, K. (2010), Topographic steering, flow recirculation, velocity redistribution, and bed topography in sharp meander bends, *Water Resour. Res.*, *46*, W09506, doi:10.1029/2009WR008303.

Blanckaert, K., and W. H. Graf (2001), Mean flow and turbulence in open-channel bend, *J. Hydraul. Eng.*, *127*, 835–847.

Blanckaert, K., and U. Lemmin (2006), Means of noise reduction in acoustic turbulence measurements, *J. Hydraul. Res.*, *44*, 3–17.

Boyer, C., A. G. Roy, and J. L. Best (2006), Dynamics of a river channel confluence with discordant beds: Flow turbulence, bed load sediment transport, and bed morphology, *J. Geophys. Res.*, *111*, F04007, doi:10.1029/2005JF000458.

Champigneulle, A., B. Buttiker, P. Durand, and M. Melhaoui (1991), Principales caractéristiques de la truite (Salmo trutta L.) dans le Léman et quelques affluents, in *La Truite, Biologie et Écologie*, (in French) edited by J. L. Baglinière and G. Maisse, pp. 153–182, INRA, Paris, France.

Dynesius, M., and C. Nilsson (1994), Fragmentation and flow regulation of river systems in the northern third of the world, *Science*, *266*, 753–762.

Dynesius, M., R. Jansson, M. E. Johansson, and C. Nilsson (2004), Intercontinental similarities in riparian-plant diversity and sensitivity to river regulation, *Ecol. Appl.*, *14*, 173–191.

Fette, M., C. Weber, A. Peter, and B. Wehrli (2007), Hydropower production and river rehabilitation: A case study on an alpine river, *Environ. Model. Assess.*, *12*, 257–267.

Formann, E., H. M. Habersack, and S. Schober (2007), Morphodynamic river processes and techniques for assessment of channel evolution in Alpine gravel bed rivers, *Geomorphology*, *90*, 340–355.

Friedl, C. (1999), Baisse de captures de poisson dans les cours d'eau suisses, in *Informations concernant la pêche*, (in french), 34 pp., Office fédéral de l'environnement, des forêts et du paysage (OFEFP), Berne, Switzerland.

Gurnell, A., N. Surian, and L. Zanoni (2009), Multi-thread river channels: A perspective on changing European alpine river systems, *Aquat. Sci.*, *71*, 253–265.

Hunziger, L. (1999), Morhology in river widenings of limited length, paper presented at 28th IAHR congress, IAHR, Graz, Austria, 22–27 August 1999.

Hurther, D., and U. Lemmin (1998), A constant-beam-width transducer for 3D acoustic Doppler profile measurements in open-channel flows, *Meas. Sci. Technol.*, *9*, 1706–1714.

Kenworthy, S. T., and B. L. Rhoads (1995), Hydrologic control of spatial patterns of suspended sediment concentration at a stream confluence, *J. Hydrol.*, *168*, 251–263.

Lake, P. S., N. Bond, and P. Reich (2007), Linking ecological theory with stream restoration, *Freshwater Biol.*, *52*, 597–615.

Lancaster, J., and B. J. Downes (2010), Linking the hydraulic world of individual organisms to ecological processes: Putting ecology into ecohydraulics, *River Res. Appl.*, *26*, 385–403.

Leclair, S., and A. G. Roy (1997), Variabilité de la morphologie et des structures sédimentaires du lit d'un confluent de cours d'eau discordant en période d'étiage, *Geogr. Phys. Quat.*, *51*, 125–139.

Leite Ribeiro, M. (2011), Influence of Tributary Widening on Confluence Morphodynamics, in *Commun. 46*, Ecole Polytech. Fédérale de Lausanne, Lausanne, Switzerland, doi:10.5075/epfl-thesis-4951.

Leite Ribeiro, M., K. Blanckaert, A. G. Roy, and A. J. Schleiss (2012), Flow and sediment dynamics in channel confluences, *J. Geophys. Res.*, *117*, F01035, doi:10.1029/2011JF002171.

Lemmin, U., and T. Rolland (1997), Acoustic velocity profiler for laboratory and field studies, *J. Hydraul. Eng.*, *123*, 1089–1098.

Lorenz, C. M., G. M. Van Dijk, A. G. M. Van Hattum, and W. P. Cofino (1997), Concepts in river ecology: Implications for indicator development, *Reg. Rivers Res. Manage.*, *13*, 501–516.

Nakamura, K., K. Tockner, and K. Amano (2006), River and wetland restoration: Lessons from Japan, *BioScience*, *56*, 419–429.

Palmer, M. A. (2009), Reforming watershed restoration: Science in need of application and applications in need of science, *Estuaries Coasts*, *32*, 1–17.

Palmer, M. A., R. F. Ambrose, and N. L. Poff (1997), Ecological theory and community restoration ecology, *Restor. Ecol.*, *5*, 291–300.

Peter, A., F. Kienast, and S. Woolsey (2005), River rehabilitation in Switzerland: Scope, challenges and research, *Arch. Hydrobiol. Suppl.*, *155*, 643–656.

Rhoads, B. L., and S. T. Kenworthy (1995), Flow structure at an asymmetrical stream confluence, *Geomorphology*, *11*, 273–293.

Rhoads, B. L., and K. D. Massey (2012), Flow structure and channel change in a sinuous grass-lined stream within an agricultural drainage ditch: Implications for ditch stability and aquatic habitat, *River Res. Appl.*, *28*(1), 39–52. doi:10.1002/rra.1430.

Rhoads, B. L., J. D. Riley, and D. R. Mayer (2009), Response of bed morphology and bed material texture to hydrological conditions at an asymmetrical stream confluence, *Geomorphology*, *109*, 161–173.

Rice, S. P., R. I. Ferguson, and T. B. Hoey (2006), Tributary control of physical heterogeneity and biological diversity at river confluences, *Can. J. Fisheries Aquat. Sci.*, *63*, 2553–2566.

Rice, S. P., P. Kiffney, C. Greene, and G. R. Pess (2008), *The Ecological Importance of Tributaries and Confluences*, pp. 209–242, John Wiley and Sons, New York.

Rohde, S. (2004), *River Restoration: Potential and limitations to re-establish riparian landscapes, Assessment and Planning*, 127 pp., Swiss Fed. Inst. of Technol. Zurich, Zurich, Switzerland.

Rohde, S., M. Schutz, F. Kienast, and P. Englmaier (2005), River widening: An approach to restoring riparian habitats and plant species, *River Res. Appl.*, *21*, 1075–1094.

Schweizer, S., M. E. Borsuk, I. Jowett, and P. Reichert (2007a), Predicting joint frequency distributions of depth and velocity for instream habitat assessment, *River Res. Appl.*, *23*, 287–302.

Schweizer, S., M. E. Borsuk, and P. Reichert (2007b), Predicting the morphological and hydraulic consequences of river rehabilitation, *River Res. Appl.*, *23*, 303–322.

Singer, M. B., and T. Dunne (2006), Modeling the influence of river rehabilitation scenarios on bed material sediment flux in a large river over decadal timescales, *Water Resour. Res.*, *42*, W12415, doi:10.1029/2006WR004894.

Weber, C. (2006), River rehabilitation and fish: The challenge of initiating ecological recovery, Ph.D. thesis, 152 pp, Swiss Fed. Inst. of Technol., Zurich, Switzerland.

Weber, C., E. Schager, and A. Peter (2009), Habitat diversity and fish assemblage structure in local river widenings: A case study on a Swiss River, *River Res. Appl.*, *25*, 687–701.

Yalin, M. S. (1971), *Theory of Hydraulic Models*, 266 pp., Macmillan Press, London.

Yalin, M. S., and A. M. F. da Silva (2001), *Fluvial Processes*, 197 pp., Int. Assoc. of Hydroenviron. Eng. and Res., Delft, Netherlands.